Green Chemistry

PAPER

View Article Online
View Journal | View Issue

Cite this: *Green Chem.*, 2017, **19**, 5203

Imidazolium-based polyionic liquid absorbents for bioproduct recovery

Stuart L. Bacon, Rachel J. Ross, Andrew J. Daugulis and J. Scott Parent*

Received 15th September 2017,
Accepted 5th October 2017

DOI: 10.1039/c7gc02806g

rsc.li/greenchem

Solid imidazolium-based polyionic liquids (PILs; a class of polyelectrolyte) were synthesized for the absorption of *n*-butanol and other inhibitory biosynthesis products from dilute aqueous solutions. Conventional hydrogels prepared by cross-linking water-soluble PILs demonstrated biocompatibility with *Saccharomyces cerevisiae*, successfully eliminating cytotoxicity concerns associated with the IL monomers. However, the cross-linked PILs' solute absorption capacity and selectivity for butanol relative to water were below the levels likely needed for a viable extractive fermentation process. Uncross-linked PILs bearing long-chain aliphatic substituents also proved to be biocompatible by virtue of their insolubility in water, and delivered significantly improved absorptive performance. Among biocompatible absorbents, these PILs demonstrated some of the highest absorptions of *n*-butanol and other hydrophilic fermentation products reported to date, with *n*-butanol partition coefficient (PC) values up to 7.6 and butanol/water selectivity ($\alpha_{b/w}$) values up to 78. The influence of linear *N*-alkyl side chain length (C_8 to C_{16}) and counter anions (Cl^-, Br^-, I^-, BF_4^-, co-SS^-) on solute partition coefficient, selectivity and physical properties are detailed and discussed. In all, this work demonstrates that polymerization of cytotoxic ILs can successfully yield biocompatible absorbents with excellent absorptive performance for the recovery of hydrophilic bioproducts.

1. Introduction

The biological synthesis of butanol from biomass has received significant attention as a means of producing renewable fuels, industrial solvents and chemical intermediates.[1–5] However, these biosyntheses frequently suffer from product inhibition at titres between 1–2 wt%,[6] leading to reduced fermentation rates, low product yields, and higher downstream recovery costs.[7] Extractive fermentation is an attractive technology in these cases, since selective absorption of a bioproduct by a second, non-aqueous phase can mitigate microorganism inhibition and improve the economics of product isolation. An ideal extractant provides a large partition coefficient for the target solute (PC_{BuOH}) and a strong preference for butanol *versus* water, as quantified by selectivity ($\alpha_{b/w} = PC_{BuOH}/PC_{water}$).[7,8]

Most extractive fermentation processes employ organic solvents as the solute sequestering phase, with oleyl alcohol being widely adopted for the recovery of ethanol and butanol. However, many small molecule absorbents present biocompatibility and water solubility limitations, as well as operational challenges stemming from volatility, foaming and emulsification.[9–12] The low vapour pressure and widely tunable composition of ionic liquids (ILs) have attracted interest for a wide range of separation processes.[13,14] Recent studies have discovered ILs capable of PC_{BuOH} far in excess of standard organic solvents,[15–17] but microbial cytotoxicity and water solubility remain critical concerns.[15,18–23] More generally, reports of IL toxicity towards a broad spectrum of organisms[24–28] and enzymes[29,30] may limit their utility for extractive fermentation.

Polymeric absorbents have emerged as promising alternatives to organic liquids, since their viscoelastic solid properties make them easy to handle, and their ability to be formulated for water insolubility can make them biocompatible.[31–34] In this work, we demonstrate these principles with a series of polyionic liquids (PILs) that are easily prepared in a wide range of compositions, provide good thermochemical stability, and demonstrate high affinity for polar organic solutes.[28,35–39] Experimental measurements of PC_{BuOH}, $\alpha_{b/w}$, Young's modulus, and biocompatibility with *Saccharomyces cerevisiae* cell cultures demonstrate the unique combination of chemical and physical properties afforded by these new extractive fermentation absorbents.

2. Experimental

2.1 Materials

1-Vinylimidazole (98%), 1-bromobutane (99%), 1-bromooctane (99%), 1-bromododecane (97%), 1-bromohexadecane (97%),

Department of Chemical Engineering, Queen's University, 19 Division St, Kingston, Ontario, Canada K7L 3N6. E-mail: scott.parent@queensu.ca

1-iodododecane (98%), 1-chlorododecane (97%), 1,10-dibromodecane (97%), sodium tetrafluoroborate ($NaBF_4$) (98%), sodium 4-styrene sulfonate (>90%), 2,2′-azobis(2-methylpropionitrile) (AIBN) (98%) and ammonium persulfate (APS) (98%) were purchased from Sigma-Aldrich (Canada). 1-Bromodecane (98%), 1-bromotetradecane (98%), sodium metabisulfite (SMBS) (97.7%) and *n*-butanol (99%) were purchased from Fischer Scientific (Canada). All chemicals were used as received. Type I ultrapure water (18.2 MΩ cm at 25 °C) was used throughout this study.

2.2 Synthesis of [VC_4Im][Br], [VC_8Im][Br], [$VC_{10}Im$][Br] and [$VC_{12}Im$][Cl]

Ionic liquid monomers were prepared as previously described[40] with minor modifications. 1-Vinylimidazole (5.00 g, 53.1 mmol) and 1.1 eq. of *n*-alkyl halide (bromobutane 8.01 g; bromooctane 11.29 g; bromodecane 12.93 g; chlorododecane 11.96 g) were dissolved in toluene (12.5 mL), heated to 90 °C and stirred for 24 h ([$VC_{12}Im$][Cl] was stirred at 100 °C for 48 h) under nitrogen. Once cooled, the upper toluene-rich phase was decanted and the oil was washed with hexanes four times. The final product was dried *in vacuo* and characterized by ^{1}H-NMR.

[VC_4Im][Br]. ^{1}H-NMR ($CDCl_3$): δ 10.95 (s, 1H), δ 7.88 (m, 1H), δ 7.61 (m, 1H), δ 7.49 (dd, 1H), δ 6.03 (dd, 1H), δ 5.40 (dd, 1H), δ 4.42 (t, 2H), δ 1.95 (m, 2H), δ 1.40 (m, 2H), δ 0.97 (t, 3H) (yield: 95%). **[VC_8Im][Br]**: ^{1}H-NMR ($CDCl_3$): δ 10.90 (s, 1H), δ 7.77 (m, 1H), δ 7.51 (dd, 1H), δ 7.47 (m, 1H), δ 5.96 (dd, 1H), δ 5.41 (dd, 1H), δ 4.42 (t, 2H), δ 1.93 (m, 2H), δ 1.26 (m, 10H), δ 0.86 (t, 3H) (yield: 70%). **[$VC_{10}Im$][Br]**: ^{1}H-NMR ($CDCl_3$): δ 11.04 (s, 1H), δ 7.78 (m, 1H), δ 7.51 (dd, 1H), δ 7.48 (m, 1H), δ 5.98 (dd, 1H), δ 5.41 (dd, 1H), δ 4.40 (t, 2H), δ 1.95 (m, 2H), δ 1.24 (m, 14H), δ 0.87 (t, 3H) (yield: 85%). **[$VC_{12}Im$][Cl]**: ^{1}H-NMR ($CDCl_3$): δ 11.32 (s, 1H), δ 7.68 (m, 1H), δ 7.56 (dd, 1H), δ 7.48 (m, 1H), δ 5.92 (dd, 1H), δ 5.41 (dd, 1H), δ 4.40 (t, 2H), δ 1.94 (m, 2H), δ 1.26 (m, 18H), δ 0.88 (t, 3H) (yield: 91%).

2.3 Synthesis of bis[VIm][Br]C_{10}

Difunctional ionic liquid cross-linker was prepared as previously described[41] with minor modifications. 1,10-Dibromodecane (3.00 g, 10.0 mmol) and 2.1 eq. of 1-vinylimidazole (1.98 g, 21.0 mmol) were dissolved in ethyl acetate (5 mL) and heated to reflux conditions under nitrogen for 36 h, stirring continuously. Once cooled, the crystal product was ground to a fine powder, washed with ethyl acetate under vacuum filtration, then dried *in vacuo* and characterized by ^{1}H-NMR.

Bis[VIm][Br]C_{10}. ^{1}H-NMR ($CDCl_3$): δ 11.13 (s, 2H), δ 7.71 (m, 2H), δ 7.68 (m, 2H), δ 7.48 (dd, 2H), δ 5.96 (dd, 2H), δ 5.42 (dd, 2H), δ 4.46 (t, 4H), δ 2.02 (m, 4H), δ 1.39 (m, 12H).

2.4 Synthesis of [$VC_{12}Im$][Br], [$VC_{14}Im$][Br], [$VC_{16}Im$][Br], [$VC_{12}Im$][I]

Ionic liquid monomers were prepared as previously described[40,42] with minor modifications. 1-Vinylimidazole (5.00 g, 53.1 mmol) and 1.1 eq. of *n*-alkyl halide (bromododecane 14.57 g; bromotetradecane 16.20 g; bromohexadecane 17.84 g; iodododecane 17.31 g) were dissolved in ethyl acetate (12.5 mL) and heated to reflux conditions under nitrogen for 24 h, stirring continuously. Once cooled, the crystal product was ground to a fine powder, washed with ethyl acetate under vacuum filtration (for **[$VC_{12}Im$][Br]** and **[$VC_{12}Im$][I]**, the flask was cooled below room temperature to induce crystallization), then dried *in vacuo* and characterized by ^{1}H-NMR.

[$VC_{12}Im$][Br]. ^{1}H-NMR ($CDCl_3$): δ 10.98 (s, 1H), δ 7.77 (m, 1H), δ 7.51 (dd, 1H), δ 7.48 (m, 1H), δ 5.96 (dd, 1H), δ 5.41 (dd, 1H), δ 4.40 (t, 2H), δ 1.95 (m, 2H), δ 1.24 (m, 18H), δ 0.87 (t, 3H) (yield: 93%, mp 44–48 °C). **[$VC_{14}Im$][Br]**: ^{1}H-NMR ($CDCl_3$): δ 11.13 (s, 1H), δ 7.69 (m, 1H), δ 7.51 (dd, 1H), δ 7.41 (m, 1H), δ 5.95 (dd, 1H), δ 5.42 (dd, 1H), δ 4.41 (t, 2H), δ 1.95 (m, 2H), δ 1.25 (m, 22H), δ 0.88 (t, 3H) (yield: 95%, mp 58 °C). **[$VC_{16}Im$][Br]**: ^{1}H-NMR ($CDCl_3$): δ 11.16 (s, 1H), δ 7.67 (m, 1H), δ 7.51 (dd, 1H), δ 7.39 (m, 1H), δ 5.94 (dd, 1H), δ 5.42 (dd, 1H), δ 4.40 (t, 2H), δ 1.96 (m, 2H), δ 1.25 (m, 26H), δ 0.88 (t, 3H) (yield: 95%, mp 66 °C). **[$VC_{12}Im$][I]**: ^{1}H-NMR ($CDCl_3$): δ 10.74 (s, 1H), δ 7.69 (m, 1H), δ 7.46 (m, 1H), δ 7.43 (dd, 1H), δ 5.98 (dd, 1H), δ 5.46 (dd, 1H), δ 4.43 (t, 2H), δ 1.97 (m, 2H), δ 1.25 (m, 18H), δ 0.88 (t, 3H) (yield: 97%, mp 49–50 °C).

2.5 Synthesis of [$VC_{12}Im$][SS] and [$VC_{12}Im$][BF_4]

IL anion metathesis was performed as previously described[40] with minor modification. **[$VC_{12}Im$][Br]** (15 g, 43.7 mmol) was slowly added to water (150 mL) at room temperature. Once dissolved, sodium 4-styrene sulfonate (11.01 g, 1.1 eq.) or sodium tetrafluoroborate (5.276 g, 1.1 eq.) was added to the mixture and stirred for 24 h at room temperature to achieve complete anion exchange, verified with ^{1}H-NMR ([$VC_{12}Im$][SS]) or ^{19}F-NMR ([$VC_{12}Im$][BF_4]) using trifluoroethanol as an internal standard. The product was extracted using dichloromethane (150 mL) then washed twice with brine solution (containing one equivalent of $NaBF_4$ or NaSS in 60 mL) then with water (60 mL). Dichloromethane was removed by vacuum. The final product was ground into a fine powder, then dried *in vacuo* and characterized by ^{1}H-NMR and ^{19}F-NMR.

[$VC_{12}Im$][SS]. ^{1}H-NMR (d-DMSO): δ 9.46 (s, 1H), δ 8.19 (m, 1H), δ 7.92 (m, 1H), δ 7.55 (d, 2H), δ 7.41 (d, 2H), δ 7.27 (m, 1H), δ 6.73 (m, 1H), δ 5.94 (dd, 1H), δ 5.83 (d, 1H), δ 5.42 (dd, 1H), δ 5.26 (d, 1H), δ 4.18 (t, 2H), 1.81 (m, 2H), 1.24 (m, 18H), 0.85 (t, 3H) (yield: 94%, mp 88–90 °C). **[$VC_{12}Im$][BF_4]**: ^{1}H-NMR ($CDCl_3$): δ 9.14 (s, 1H), δ 7.63 (m, 1H), δ 7.41 (m, 1H), δ 7.15 (dd, 1H), δ 5.82 (dd, 1H), δ 5.40 (dd, 1H), δ 4.26 (t, 2H), δ 1.90 (m, 2H), δ 1.25 (m, 18H), δ 0.88 (t, 3H). ^{19}F-NMR ($CDCl_3$): δ −151.97 (s, 4F, $^{11}BF_4$), δ −152.02 (s, 4F, $^{10}BF_4$) (yield: 80%, mp 37–40 °C).

2.6 Synthesis of P(VC_4ImBr) and P(VC_{12}ImBr) with APS initiator (methanol/water)

Polymerization was performed as described elsewhere with minor modification.[42] Varying quantities of monomer ([VC_4Im][Br] or [$VC_{12}Im$][Br]) and cross-linker bis(vinylimidazolium bromide)decane (**bis[VIm][Br]C_{10}**), with a combined

mass of 5 g, were dissolved in methanol (2 mL) and water (0.75 mL) with ammonium persulfate (APS; 0.03 mol-initiator/mol-monomer) at room temperature. Sodium *meta*-bisulfite (SMBS; 0.03 mol-initiator/mol-monomer) in water (0.4 mL) was added to the reaction mixture and allowed to react for 24 h at room temperature. **P(VC$_4$ImBr)** was precipitated in excess acetone, dried *in vacuo* at 60 °C and was characterized by ^{1}H-NMR. **P(VC$_{12}$ImBr)** precipitated during polymerization and was washed several times in Type I ultrapure water and was characterized by ^{1}H-NMR. Uncross-linked hydrated monolithic material was pressed in a Wabash press at 30 °C for 12 h to prepare a bulk solid. **P(VC$_4$ImBr)** and **P(VC$_{12}$ImBr)** thermosets containing the cross-linker **bis[VIm][Br]C$_{10}$** were washed several times in Type I ultrapure water, however, they did not dissolve and could not be characterized by ^{1}H-NMR.

P(VC$_4$ImBr). ^{1}H-NMR ($CDCl_3$): δ 10.02 (br, 1H), δ 8.42 (br, 1H), δ 7.19 (br, 1H), δ 4.96 (br, 1H), δ 4.26 (br, 2H), δ 2.31 (br, 2H), δ 1.97 (br, 2H), δ 1.45 (br, 2H), δ 1.01 (br, 3H).

P(VC$_{12}$ImBr). ^{1}H-NMR ($CDCl_3$): δ 9.95 (br, 1H), δ 8.37 (br, 1H), δ 7.19 (br, 1H), δ 4.89 (br, 1H), δ 4.21 (br, 2H), δ 2.07 (br, 4H), δ 1.28 (br, 18H), δ 0.90 (br, 3H).

2.7 Synthesis of P(VC$_8$ImBr), P(VC$_{10}$ImBr), P(VC$_{12}$ImBr), P(VC$_{14}$ImBr), P(VC$_{16}$ImBr), P(VC$_{12}$ImCl), P(VC$_{12}$ImI), P(VC$_{12}$ImBF$_4$) and P(VC$_{12}$Im-*co*-SS) with AIBN initiator (toluene/ethanol)

Bulk polymerization was performed as described elsewhere with minor modification.[42] The required monomer (5 g) was dissolved in a 9 : 1 toluene : ethanol mixture (25 mL) at room temperature. 2,2′-Azobis(2-methylpropionitrile) (AIBN; 0.03 mol-initiator/mol-monomer) was added to the mixture and stirred at room temperature until dissolved. The temperature was increased to 90 °C, and heating continued under nitrogen and reflux for 5 h. Once cooled to room temperature, the polymer was precipitated from excess acetone (methanol was used to precipitate **P(VC$_{12}$ImBF$_4$)**) and allowed to settle. **P(VC$_{12}$Im-*co*-SS)** was completely insoluble in every solvent tested and was therefore purified by simply washing with acetone. In all cases, the acetone was decanted after 24 h and fresh acetone was added. Acetone was decanted after another 24 h, and the final product was dried *in vacuo* and characterized by ^{1}H-NMR.

P(VC$_8$ImBr). ^{1}H-NMR ($CDCl_3$): δ 10.06 (br, 1H), δ 8.51 (br, 1H), δ 7.11 (br, 1H), δ 4.91 (br, 1H), δ 4.21 (br, 2H), δ 2.10 (br, 2H), δ 1.98 (br, 2H), δ 1.29 (br, 10H), δ 0.89 (br, 3H). **P(VC$_{10}$ImBr)**: ^{1}H-NMR ($CDCl_3$): δ 10.06 (br, 1H), δ 8.54 (br, 1H), δ 7.10 (br, 1H), δ 4.94 (br, 1H), δ 4.21 (br, 2H), δ 1.95 (br, 4H), δ 1.27 (br, 14H), δ 0.89 (br, 3H). **P(VC$_{12}$ImBr)**: ^{1}H-NMR ($CDCl_3$): δ 9.95 (br, 1H), δ 8.37 (br, 1H), δ 7.19 (br, 1H), δ 4.89 (br, 1H), δ 4.21 (br, 2H), δ 2.07 (br, 4H), δ 1.28 (br, 18H), δ 0.90 (br, 3H). **P(VC$_{14}$ImBr)**: ^{1}H-NMR ($CDCl_3$): δ 9.97 (br, 1H), δ 8.37 (br, 1H), δ 7.15 (br, 1H), δ 4.90 (br, 1H), δ 4.20 (br, 2H), δ 2.11 (br, 2H), δ 1.98 (br, 2H), δ 1.26 (br, 22H), δ 0.89 (br, 3H). **P(VC$_{16}$ImBr)**: ^{1}H-NMR ($CDCl_3$): δ 9.95 (br, 1H), δ 8.35 (br, 1H), δ 7.14 (br, 1H), δ 4.88 (br, 1H), δ 4.22 (br, 2H), δ 2.05 (br, 4H), δ 1.27 (br, 26H), δ 0.89 (br, 3H). **P(VC$_{12}$ImCl)**: ^{1}H-NMR ($CDCl_3$): δ 10.13 (br, 1H), δ 8.61 (br, 1H), δ 7.12 (br, 1H), δ 4.87 (br, 1H), δ 4.21 (br, 2H), δ 2.16 (br, 2H), δ 1.96 (br, 2H), δ 1.28 (br, 18H), δ 0.90 (br, 3H). **P(VC$_{12}$ImI)**: ^{1}H-NMR ($CDCl_3$): δ 9.95 (br, 1H), δ 8.37 (br, 1H), δ 7.19 (br, 1H), δ 4.89 (br, 1H), δ 4.21 (br, 2H), δ 2.07 (br, 4H), δ 1.28 (br, 18H), δ 0.90 (br, 3H). **P(VC$_{12}$ImBF$_4$)**: ^{1}H-NMR ($CDCl_3$): δ 8.49 (br, 1H), δ 7.21 (br, 2H), δ 4.09 (br, 3H), δ 1.79 (br, 4H), δ 1.27 (br, 18H), δ 0.89 (br, 3H). ^{19}F-NMR ($CDCl_3$): δ −151.97 (s, 4F, $^{11}BF_4$), δ −152.02 (s, 4F, $^{10}BF_4$). **P(VC$_{12}$ImSS)**: would not dissolve.

2.8 Partition coefficient and selectivity experiments

PIL absorptive properties were quantified by determining the solute partition coefficient (PC_i) and selectivity in triplicate, as previously described.[28] A 5 wt% polymer phase fraction was used throughout, with initial aqueous solute concentrations between 5 g L^{-1} to 50 g L^{-1} depending on reported inhibitory concentrations. Aqueous solute concentrations before and after equilibration with the polymer were measured using a Varian 450-GC gas chromatography unit equipped with a CP-8410 AutoInjector, VF-5 ms 30 m capillary column and FID detector. Equilibration times varied based on polymer properties and physical dimensions and was determined by time-trial experiments.

Equilibrated polymer samples (~0.10 ± 0.02 g; triplicate) were lightly pat dry with a paper towel and dried in aluminum weigh pans to determine total water/solute uptake. Samples were dried at 60 °C and weighed every 12 hours until the polymer mass remained unchanged between time intervals.

A mass balance was performed to determine the solute and water concentration in the polymer phase. Experimental partition coefficient (PC) and selectivity ($\alpha_{i/w}$) values were calculated using aqueous and polymer phase weight fractions (w_i^{aq} and w_i^{poly}) of the solute and water in eqn (1). Standard deviation values were calculated from triplicate samples to establish a mean value for the equilibrium PC.

$$PC_i = \frac{w_i^{poly}}{w_i^{aq}} \quad (1)$$

Solute/water selectivity ($\alpha_{i/w}$) was calculated as in eqn (2).

$$\alpha_{i/w} = \frac{PC_i}{PC_w} \quad (2)$$

2.9 Young's modulus (*E*)

After equilibration with an aqueous solution, polymer samples were lightly dried with a paper towel and assayed in triplicate using a Shore A durometer on a flat level bench at room temperature. In cases where materials fragmented, durometer readings were taking immediately prior to fracture. Young's modulus (*E*; MPa) was estimated from durometer readings as previously described.[43]

2.10 Polymer imaging

Dry polymer samples were fractured in liquid nitrogen, gold-coated and imaged using a Hitachi S-2300 scanning electron

microscope at 600× and 2000× magnification. Images were analyzed using ImageJ software.

2.11 Biocompatibility testing

Saccharomyces cerevisiae was obtained from Alltech (Nicholasville, Kentucky) and cultivated in a medium from Doran and Bailey[44] containing 10 g L^{-1} glucose, 5 g L^{-1} KH_2PO_4, 2 g L^{-1} yeast extract, 2 g L^{-1} $(NH_4)_2SO_4$, 0.4 g L^{-1} $MgSO_4{\cdot}7\ H_2O$, and 0.1 g L^{-1} $CaCl_2$. Polymer biocompatibility was determined as previously described.[28] Briefly, 50 mL of freshly prepared growth medium was added to 125 mL Erlenmeyer flasks and sterilized by autoclave. Once cool, 5 g of sterile polymer or IL monomer was aseptically added to the flasks, inoculated with 2 mL of −80 °C glycerol stock culture and incubated at 180 rpm and 30 °C for 24 h. Cell growth was determined through triplicate optical density measurements at 600 nm (OD_{600}) using a Biochrom Ultrospec 3000 UV/Visible Spectrophotometer and compared to duplicate control cultures. **[VC_{16}Im][Br]** formed a stable emulsion with the fermentation medium and could not be evaluated using this method.

3. Results and discussion

3.1 Biocompatibility

Extractants are classified as biocompatible if they do not adversely affect microbial growth when placed in direct contact with cells in a fermentation medium. This is typically assessed by monitoring cell proliferation within a suspended culture exposed to 10 wt% of the non-aqueous phase.[45–47] In the present study, biocompatibility was quantified by measurement of the optical density (600 nm) of *Saccharomyces cerevisiae*, an industrial ethanol-producing yeast and an important vehicle for genetic engineering that can be manipulated to produce *n*-butanol or iso-butanol.[48–50]

The optical density data plotted in Fig. 1 show that all the ILs used in this work are cytotoxic towards *S. cerevisiae*, as they severely inhibited suspended cell growth (relative $OD_{600} < 0.15$) compared to the single-phase control. These results align with previous reports of imidazolium IL cytotoxicity towards a range of microorganisms.[21,22,24] Polymerizing the relatively hydrophilic monomer, **[VC_4Im][Br]**, yielded a water-soluble polyelectrolyte **P(VC_4ImBr)** that also inhibited *S. cerevisiae* growth, albeit to a lesser extent than the small molecule IL (relative $OD_{600} \sim 0.50$). This cytotoxicity, combined with the obvious material handling issues associated with a water-soluble material, requires absorbent PILs to be rendered immiscible with water, either through extensive crosslinking to yield a hydrogel, or by altering composition such that its dissolution in water is thermodynamically unfavorable.

This is illustrated in Fig. 1 by optical density measurements recorded for cross-linked copolymers of **[VC_4Im][Br]** with the difunctional IL monomer **bis[VIm][Br]C_{10}**. Whereas the linear, water-soluble PIL, **P(VC_4ImBr)**, was cytotoxic, its cross-linked hydrogel analogues were biocompatible with *S. cerevisiae*, irrespective of crosslink density. An alternate approach to water in-

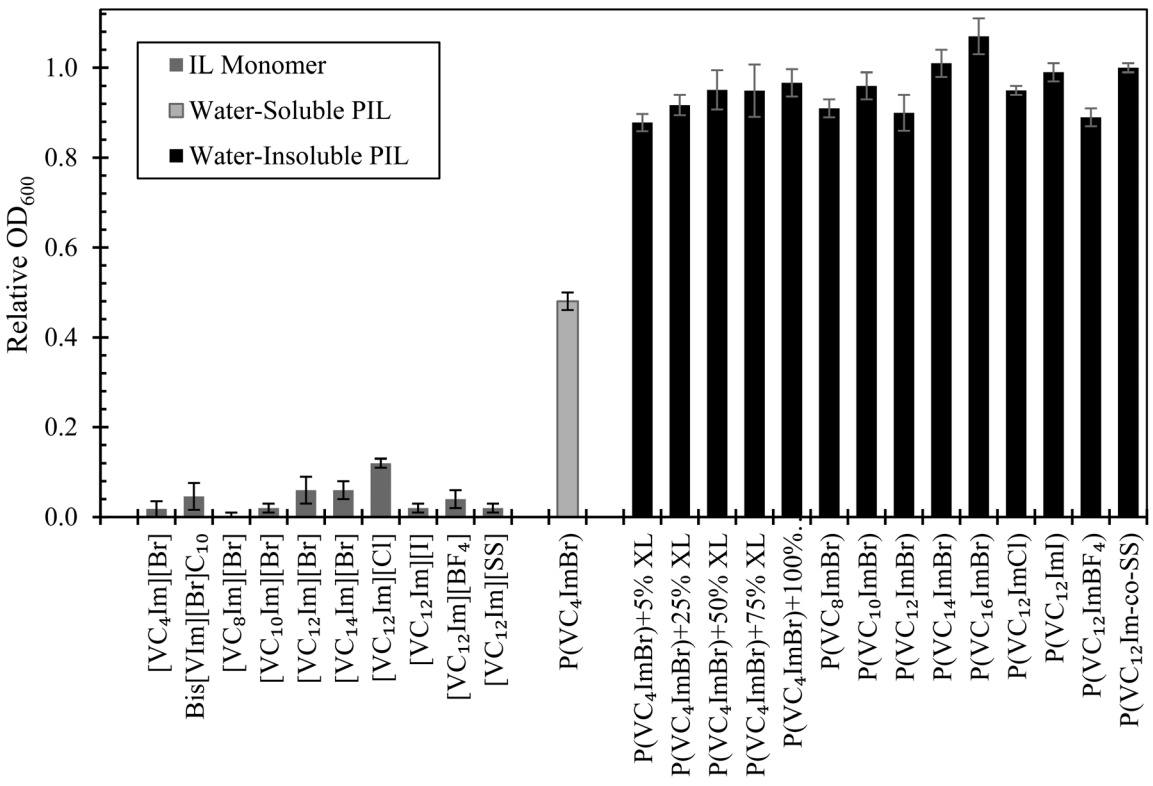

Fig. 1 Optical density (OD_{600}) of *S. cerevisiae* cultures containing 10 wt% IL monomer or PIL relative to a single phase control after 24 h.

soluble PILs involves the use of larger *N*-alkyl substituents that render the material more hydrophobic, as demonstrated by the biocompatibility of materials bearing C_8–C_{16} linear aliphatic groups. In all, these results demonstrate that polymerization can be an effective means to reduce or eliminate cytotoxicity concerns associated with IL extractants, and highlight a promising class of absorbents for partitioning bioreactor applications.

3.2 Hydrogel formulations

Having established that PILs can be rendered biocompatible, our assessments shifted to other properties of an extractive fermentation absorbent: solute affinity and material strength. Note that a solid absorbent must withstand the forces exerted by stirred-tank bioreactors and ensuing solid–liquid separation operations. Here, durometry measurements were translated into Young's modulus (E) data, which are reported widely for polymeric materials as a measure of its elastic resistance to an applied deformation.[51] The data in Fig. 2a reveal the effect of cross-link density on hydrogel stiffness. As expected, a low cross-linker content produced relatively weak material (5 wt% **bis[VIm][Br]C_{10}**; E = 0.9 ± 0.2 MPa), due in large part to a high degree of swelling. This is indicated by the high liquid fraction within this hydrogel ($w^{poly}_{BuOH} + w^{poly}_{H_2O} = 900\,g\,kg^{-1}$; Fig. 2b) which can be rectified by raising the copolymer's difunctional monomer content and, by extension, the hydrogel's crosslink density.

The efficacy of an absorbent toward a solute is quantified by partition coefficients (PC_{BuOH}) and the solute/water selectivity ($\alpha_{b/w} = PC_{BuOH}/PC_{H_2O}$). The higher the PC_{BuOH} value, the less bioreactor volume that must be occupied by the polymer to satisfy a solute concentration target. A higher selectivity value raises the solute concentration in the polymer phase relative to that of water, thereby reducing downstream product recovery costs.[52] The effect of hydrogel cross-link density on PC_{BuOH} and $\alpha_{b/w}$ is illustrated in Fig. 2c and d, respectively. The data show that increasing cross-link density improves PC_{BuOH} from 0.75 to 1.2. Similarly, the more tightly cross-linked networks absorbed lower amounts of water, yielding nearly 6-fold improvements in $\alpha_{b/w}$ from 0.75 to 4.4.

Unfortunately, these values fall well short of known extractive fermentation absorbents. For reference, oleyl alcohol is a biocompatible organic solvent that provides an *n*-butanol PC of 3.6 ± 0.4 and $\alpha_{b/w}$ = 180 ± 53.[15,52–54] In general, the hydrophilicity of PIL hydrogels resulted in a preferential affinity for water over *n*-butanol, requiring a shift in material composition to instill a more hydrophobic character.

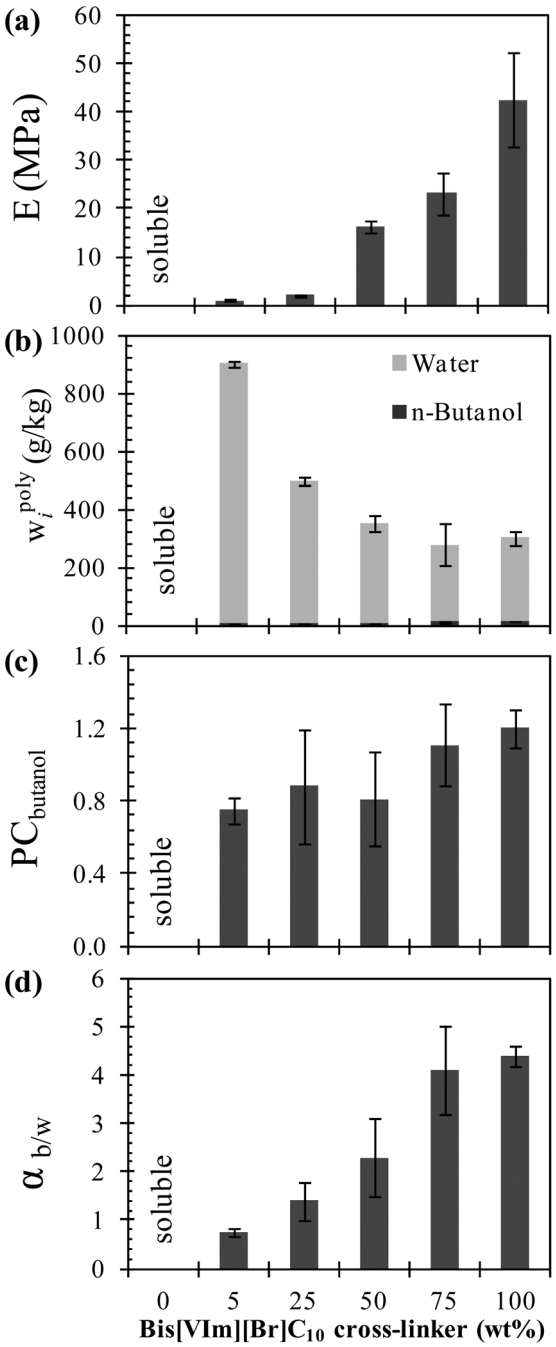

Fig. 2 Properties of **P(VC_4ImBr)** gels containing varying amounts of **bis[VIm][Br]C_{10}** cross-linker (10 g L^{-1} initial *n*-butanol concentration; 5 wt% polymer phase fraction; 30 °C).

3.3 Hydrophobic formulations-monoliths

Unlike our linear and crosslinked PILs bearing a C_4 substituent, **P(VC_{12}ImBr)** is a linear homopolymer that does not dissolve in water, despite the fact that its monomer, **[VC_{12}Im][Br]**, has appreciable water solubility. This solubility difference between IL monomer and polymer has important implications in terms of biocompatibility, extractant losses and bioproduct isolation, and stems from differences in the thermodynamics of mixing. In thermodynamic terms, an extractant is immiscible with water if the pair possess a positive Gibbs energy of mixing, which is comprised of enthalpic and entropic contributions ($\Delta G_{mix} = \Delta H_{mix} - T\Delta S_{mix}$).

Given that the entropy (ΔS_{mix}) generated by dissolving a monomer far exceeds that produced by a polymer, lower molecular weight compounds generally support miscibility to a greater extent than polymeric materials.[34] The observed insolu-

bility of **P(VC$_{12}$ImBr)** in water ($\Delta G_{mix} > 0$) resulted from the polymer's small entropy of mixing being unable to overcome the system's significant, positive enthalpy of mixing (indicative of unfavorable polymer–water interactions). In contrast, a larger ΔS_{mix} generated by monomer + water resulted in partial aqueous solubility ($G_{mix} < 0$). Changes to chemical structure *via* polymerization can affect ΔH_{mix} and, by extension, miscibility. However, water solubility limit estimates[55] of 1-vinylimidazole (26.6 g L^{-1}) and 1-ethylimidazole (26.2 g L^{-1}) indicate that the conversion of vinyl to alkyl functionality likely had a limited effect on ΔH_{mix}.

The hydrophilic structure of **P(VC$_4$ImBr)** enabled more favorable polymer + water interactions (indicated by a small positive or negative enthalpic term) which, combined with a small entropic contribution, resulted in polymer/water miscibility ($\Delta G_{mix} < 0$). In all, these findings highlight the sensitivity of polymer + solute interactions towards ΔS_{mix} and ΔH_{mix}. In previous studies,[34,56,57] we utilized thermodynamic activity models (*e.g.* UNIFAC-vdW-FV) to predict solute absorption in non-ionic polymers, providing a basis for material selection and design. However, given the current state of knowledge, first-principles estimation of PIL + solute affinity is unavailable, making the material development process largely empirical.

Phase equilibria also affected our initial series of **P(VC$_{12}$ImBr)** preparations, which involved the polymerization of **[VC$_{12}$Im][Br]** in methanol/water. Starting from a miscible condition, redox initiation of the radical process gave rise to precipitation polymerization,[58,59] due to the decrease in solubility associated with growing polymer chains. The product emerged as a monolith comprised of fused spheres with diameters of 1 to 3 μm (Fig. 3). The high surface area and void fraction provided by this morphology has been reported for related imidazolium-based PILs,[60,61] and can be advantageous in applications such as chromatography. However, in the context of extractive fermentation, these microporous structures are generally undesirable. High surface area solids are prone to fouling, and the filling of interstitial voids with fermentation medium is non-selective for the bioproduct *versus* water.

Consider the data listed in Table 1, which describe butanol uptake by various **P(VC$_{12}$ImBr)** absorbents. The monolithic solids took up much greater quantities of water compared to a corresponding continuous solid, resulting in significantly reduced modulus values. While this material stiffness deficiency was overcome by incorporating difunctional monomer to produce crosslinked monoliths, fluid uptake by pores was non-selective, generating $\alpha_{b/w}$ five times lower than those provided by bulk material (compressed monolith). These data confirm that solute absorption occurred primarily throughout the material's bulk, with no apparent benefit of preparing high surface area solids. Moreover, linear, thermoformable materials are more attractive than thermosets, as they are amenable to processing/recycling by standard polymer processing techniques.

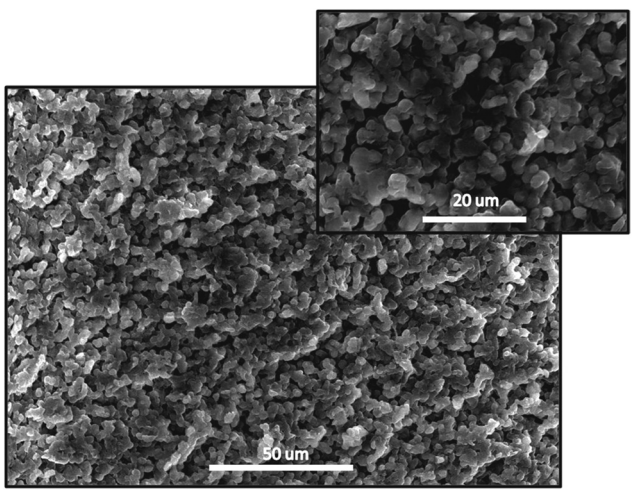

Fig. 3 Monolith structure of **P(VC$_{12}$ImBr)** containing 10 wt% **bis [VIm][Br]C$_{10}$** cross-linker.

3.4 Hydrophobic formulations-bulk solids

Polymerization of **[VC$_{12}$Im][Br]** using AIBN in toluene/ethanol is a conventional solution process, from which **P(VC$_{12}$ImBr)** is isolated by precipitation from excess acetone. The bulk polymer's affinity for butanol and water are indistinguishable from that of a compressed monolith (Table 1), with PC_{BuOH} = 6.7 ± 0.5 and $\alpha_{b/w}$ = 58 ± 5. These values rank among the best thermodynamic affinities of any biocompatible absorbent reported to date, as the observed PC_{BuOH} is nearly twice that of oleyl alcohol. The physical properties of solution-polymerized **P(VC$_{12}$ImBr)** are also noteworthy, as the hydrated material produced a high Young's modulus and could be thermoformed at mild temperatures using conventional polymer processing equipment. Therefore, this synthetic procedure was used throughout the remainder of the study.

The influence of *n*-alkyl chain length on PIL properties was examined for substituents ranging from C_8 to C_{16}. The data

Table 1 Properties of **P(VC$_{12}$ImBr)** absorbents (10 g L^{-1} initial *n*-butanol concentration; 5 wt% polymer phase fraction; 30 °C)

Initiator (medium)	Cross-linker[a] (wt%)	Product morphology	*E* (MPa)	w^{poly}_{BuOH} (g kg^{-1})	$w^{poly}_{H_2O}$ (g kg^{-1})	PC_{BuOH}	$\alpha_{b/w}$
APS (methanol/water)	—	Monolith	4.5 ± 0.4	34 ± 5	450 ± 20	4.4 ± 0.8	10 ± 2
APS (methanol/water)	5	Monolith	7.6 ± 0.2	34 ± 2	440 ± 19	4.3 ± 0.3	10 ± 1
APS (methanol/water)	10	Monolith	14.0 ± 1.0	33 ± 2	385 ± 9	4.1 ± 0.3	11 ± 2
APS (methanol/water)	—	Compressed monolith	8.8 ± 1.0	47 ± 2	120 ± 2	6.7 ± 0.5	56 ± 5
AIBN (toluene/ethanol)	—	Continuous bulk	17.2 ± 2.0	51 ± 3	125 ± 4	6.9 ± 0.3	56 ± 4

[a] **Bis[VIm][Br]C$_{10}$**.

plotted in Fig. 4a and b show that material stiffness and absorbed liquid content are highly sensitive to substituent length. The more hydrophilic, short-chain PILs absorbed more water, resulting in greater plasticization of the solid, and lower modulus values. Interestingly, the total amount of *n*-butanol absorbed was constant amongst the C_8 to C_{14} materials – only the amount of absorbed water changed. Butanol partition coefficients remained nearly constant (Fig. 4c), but butanol/water selectivity improved significantly over this limited range (Fig. 4d).

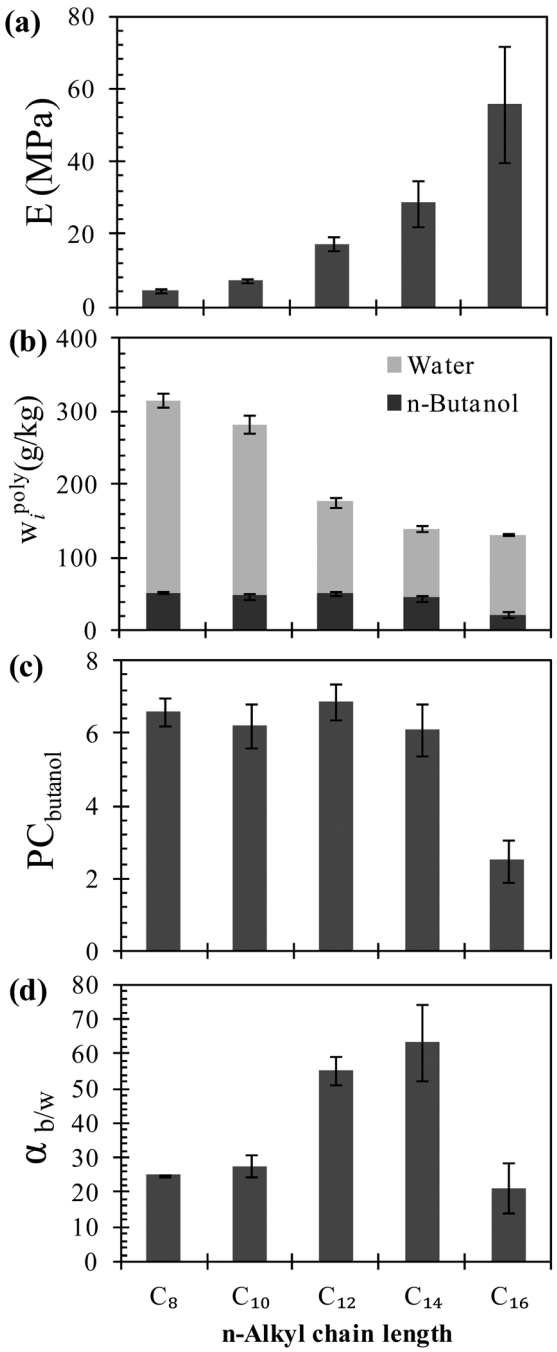

Fig. 4 Effect of imidazolium substituent *n*-alkyl chain length on **P(VC$_{\#}$ImBr)** properties (10 g L^{-1} initial *n*-butanol concentration; 5 wt% polymer phase fraction; 30 °C).

The sharp change in material properties observed on moving from C_{14} to C_{16} was unexpected, and seems to establish an upper limit for *n*-alkyl length. The C_8 to C_{14} polymers were flexible and durable in a hydrated state, whereas the C_{16} material, despite its large modulus, fractured and crumbled under applied strain. In a dry state, the C_{16} polymer was opaque and white, an indicator of semi-crystalline morphology, and notably different than the transparent C_8 to C_{14} materials. Differential scanning calorimetry analysis of **P(VC$_{16}$ImBr)** revealed a melting endotherm at 172 °C, consistent with a limited extent of side-chain crystallization. As absorption is typically limited to amorphous domains,[57,62] the observed crystallinity may account for the material's decreased PC_{BuOH}.

In addition to alkyl chain length, the PIL counter anion provides a means of tuning material properties to satisfy modulus, PC_{BuOH} and $\alpha_{b/w}$ targets. The data plotted in Fig. 5 illustrate differences between **P(VC$_{12}$ImX)** polyelectrolytes bearing a range of anions (Cl^-, Br^-, I^- BF_4^- and co-SS^-). Relative hydrophobicity of the Cl^-, Br^-, I^- and BF_4^- can be assessed with the Hofmeister series, which quantifies a dissociated ion's ability to precipitate proteins from aqueous solution.[63,64] According to this scale, hydrophobicity varies as follows: $Cl^- < Br^- < I^- < BF_4^-$. Of the four PILs tested, the most hydrophobic, **P(VC$_{12}$ImBF$_4$)**, provided the lowest PC_{BuOH}, in combination with a middling selectivity. The homologous series of halide-bearing PILs is more revealing. Consistent with our observations for *n*-alkyl chain length, an increase in halide hydrophobicity lowered total liquid absorption levels. By extension, modulus values improved in response to a lower extent of solid plasticization. Selectivity also responded positively to heightened hydrophobicity, as **P(VC$_{12}$ImI)** provided the highest value recorded in this work ($\alpha_{b/w}$ = 78 ± 15). However, anion effects were such that an increase in hydrophobic character reduced the observed partition coefficient (PC_{BuOH} = 7.6 ± 0.7 for **P(VC$_{12}$ImCl)** *versus* 3.8 ± 0.5 for **P(VC$_{12}$ImI)**). This suggests that the choice of halide requires a balance between PC_{BuOH}, which dictates the amount of polymer needed to reduce butanol concentrations below inhibitory levels, and $\alpha_{b/w}$, which dictates the ease of isolating pure butanol from the polymer phase.

A potential limitation of PILs in bioproduct recovery applications is the possibility of anion/cation exchange with the fermentation medium. In response to this concern, the polyampholyte **P(VC$_{12}$Im-*co*-SS)** was synthesized through copolymerization of 1-vinyl-3-dodecylimidazolium and 4-styrene sulfonate. It is anticipated that the entangled polyanion chains are kinetically limited from large scale anion metathesis, mitigating *in situ* ion metathesis concerns. This polymer also provided good separation of *n*-butanol, with PC_{BuOH} = 4.5 ± 0.5 and $\alpha_{b/w}$ = 36.1 ± 4.3. Further investigation is required to evaluate the prevalence of PIL ion exchange in representative fermentation medium, as well as evaluating further polycation-

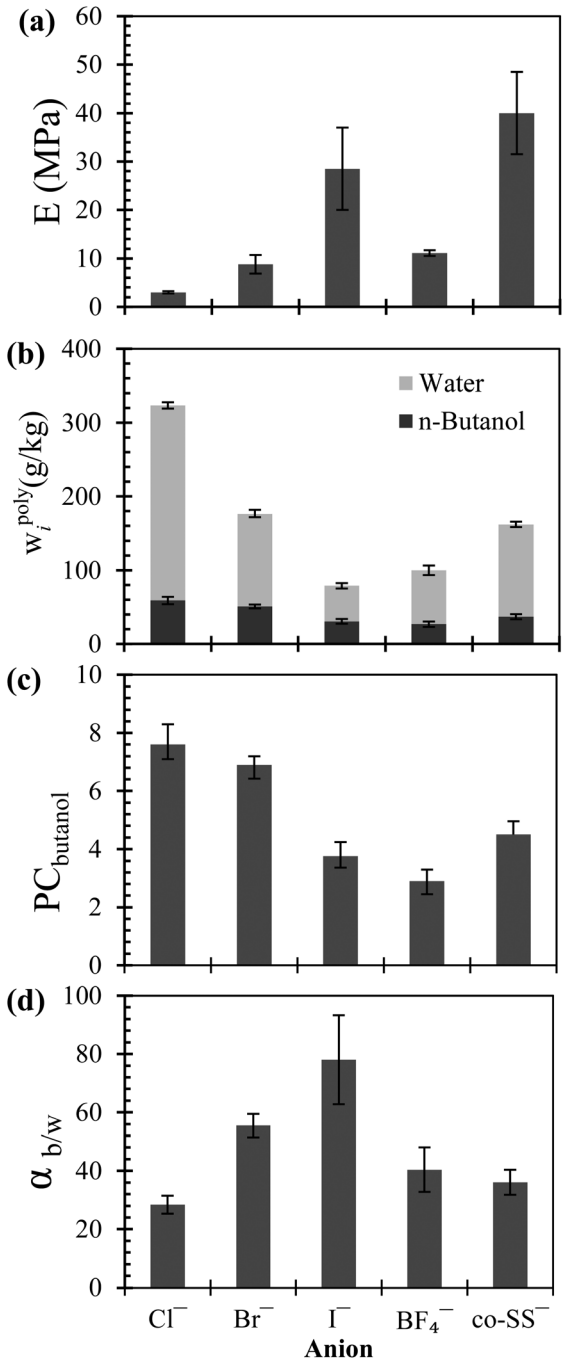

Fig. 5 Effect anion structure on **P(VC$_{12}$ImX)** properties (10 g L^{-1} initial *n*-butanol concentration; 5 wt% polymer phase fraction; 30 °C).

co-polyanion polymers to improve absorptive physical properties.

Direct comparison of our PILs with analogous ILs is prevented by the miscibility of dialkylimidazolium halide ILs with water.[65] More hydrophobic ILs can phase split, but generally possess poor butanol affinity, with reported metrics (PC_{BuOH}; $\alpha_{b/w}$) for 1-octyl-3-methylimidazolium salts as follows: [OMIm][BF_4] (2.2–2.7; 12–19), [OMIm][PF_6] (0.9–1.1; 49–55), [OMIm][Tf_2N] (1.4–1.5; 80–135), [OMIm][TfO] (1.0; 3.6), [OMIm][TCB] (3.0; 73), [OMIm][TCM] (4.7; 35).[17,54,66,67] Aside from imidazolium ILs, other chemistries including tetraalkylammonium[15,16] and tetraalkylphosphonium[16] have been demonstrated to provide PC values up to 21, and $\alpha_{b/w}$ up to 274, however, cell biocompatibility was not tested. Nonetheless, these reports suggest that significant room exists for further optimization of PIL performance, provided that biocompatibility, physical property and thermochemical stability demands are met.

3.5 Extractive fermentation applications

Butanol recovery from a solid polymer phase can be achieved using techniques developed for adsorptive processes, such as thermal/vacuum desorption or solute extraction into an appropriate solvent (*i.e.* methanol), followed by a finishing distillation step.[68] Solid, thermoplastic polymers are well suited for these applications due to their negligible vapour pressure and mechanical strength. Recovering butanol from dilute aqueous solution is complicated by a heterogeneous azeotrope at 57.3 wt% *n*-butanol (92.3 °C),[69] which prevents the downstream isolation of pure alcohol using a single distillation column. A PIL extractant capable of concentrating butanol from the aqueous phase to exceed the azeotropic composition is, therefore, very attractive. The composition of the polymer phase is a function of the selectivity of the PIL for butanol and the maximum tolerable concentration of alcohol in the fermentation medium. Assuming that a bioprocess can accommodate 1 wt% butanol in the aqueous phase, a PIL must provide butanol $\alpha_{b/w}$ = 133 to reach the azeotrope. If the microorganism can tolerate 1.5 wt% butanol, the required $\alpha_{b/w}$ falls to 88, while a 2 wt% butanol tolerance requires $\alpha_{b/w}$ = 66. This simple relationship underscores the importance of continued improvements in microbe solvent tolerance through genetic engineering.[6]

Note that PC_{BuOH} does not factor into these downstream recovery considerations, but directly affects the volumetric productivity of a bioreactor, since a higher absorption capacity means that less polymer is needed to produce the target butanol concentration. Based on available data, **P(VC$_{12}$ImI)** is the best PIL developed to this point, due to its high *n*-butanol selectivity ($\alpha_{b/w}$ = 78; PC_{BuOH} = 3.8). The equilibrium experiment that generated these data produced an aqueous phase containing 0.81 wt% butanol, and a polymer phase whose absorbed liquid composition was 39 wt% *n*-butanol. This falls short of the azeotropic composition, however, the sensitivity of PC and $\alpha_{b/w}$ towards cation and anion composition encourages further PIL optimization.

Several other fermentation processes, including the bioproduction of ethanol, iso-butanol, acetone and 2,3-butanediol also suffer from end-product inhibition. Table 2 demonstrates the performance of PILs toward a range of polar bioproducts, with **P(VC$_{12}$ImBr)** providing PC values significantly better than oleyl alcohol, albeit with lower $\alpha_{o/w}$ values. As each bioprocess may possess varying economic sensitivity to PC and $\alpha_{b/w}$, bioprocess-specific targets should be defined for further material design and optimization.

Table 2 Sorption of molecules pertinent to extractive fermentation

	Initial solute concentration ($g\ L^{-1}$)	PC	$\alpha_{i/w}$	E (MPa)
P(VC_{12}ImBr)				
n-Butanol	10	6.9 ± 0.5	56 ± 4	17.2 ± 1.9
Iso-butanol	10	5.6 ± 0.4	40 ± 4	18.8 ± 3.4
Ethanol	10	1.1 ± 0.3	7 ± 2	27.4 ± 8.2
Acetone	5	0.7 ± 0.3	5 ± 2	29.3 ± 5.4
Water	1000	0.14 ± 0.01	—	31.2 ± 8.5
2,3-Butanediol	50	1.1 ± 0.1	8 ± 1	25.1 ± 2.6
Oleyl alcohol				
n-Butanol	10	3.6 ± 0.4	180 ± 53	n/a
Iso-butanol	10	2.7 ± 0.4	135 ± 29	n/a
Ethanol	10	0.30 ± 0.08	24 ± 7	n/a

4. Conclusions

Absorbent PILs produced from vinylimidazolium IL monomers were biocompatible with *S. cerevisiae* by virtue of their insolubility in water, achieved through copolymerization with a difunctional monomer (cross-linker) or incorporation of a long chain (C_8 to C_{16}) aliphatic substituent. PIL biocompatibility was in sharp contrast to the IL monomers, which severely inhibited *S. cerevisiae* growth. Most PILs studied were durable solids, with Young's modulus values between 3 to 56 MPa after equilibration with a 1 wt% *n*-butanol aqueous solution. The PILs demonstrated an ability to absorb and enrich *n*-butanol and other fermentation products. Absorptive properties were sensitive towards *N*-alkyl side chain length and counter anion (Cl^-, Br^-, I^-, BF_4^-, co-SS^-), with *n*-butanol PC values up to 7.6 and *n*-butanol/water selectivity ($\alpha_{b/w}$) up to 78. A high surface area monolithic PIL structure was also prepared, however, demonstrated significantly lower PC_{BuOH}, $\alpha_{b/w}$ and modulus values than comparable bulk solids due to non-selective filling of the interstitial pores.

List of abbreviations

[VC_4Im][Br]	1-Vinyl-3-butylimidazolium bromide
[VC_8Im][Br]	1-Vinyl-3-octylimidazolium bromide
[VC_{10}Im][Br]	1-Vinyl-3-decylimidazolium bromide
[VC_{12}Im][Br]	1-Vinyl-3-dodecylimidazolium bromide
[VC_{14}Im][Br]	1-Vinyl-3-tetradecylimidazolium bromide
[VC_{16}Im][Br]	1-Vinyl-3-hexadecylimidazolium bromide
[VC_{12}Im][Cl]	1-Vinyl-3-dodecylimidazolium chloride
[VC_{12}Im][I]	1-Vinyl-3-dodecylimidazolium iodide
[VC_{12}Im][BF_4]	1-Vinyl-3-dodecylimidazolium tetrafluoroborate
[VC_{12}Im][SS]	1-Vinyl-3-dodecylimidazolium 4-styrene sulfonate
Bis[VIm][Br]C_{10}	Bis(vinylimidazolium bromide)decane
P(VC_4ImBr)	Poly(vinylbutylimidazolium bromide)
P(VC_8ImBr)	Poly(vinyloctylimidazolium bromide)
P(VC_{10}ImBr)	Poly(vinyldecylimidazolium bromide)
P(VC_{12}ImBr)	Poly(vinyldodecylimidazolium bromide)
P(VC_{14}ImBr)	Poly(vinyltetradecylimidazolium bromide)
P(VC_{16}ImBr)	Poly(vinylhexadecylimidazolium bromide)
P(VC_{12}ImCl)	Poly(vinyldodecylimidazolium chloride)
P(VC_{12}ImI)	Poly(vinyldodecylimidazolium iodide)
P(VC_{12}ImBF_4)	Poly(vinyldodecylimidazolium tetrafluoroborate)
P(VC_{12}Im-*co*-SS)	Poly(vinyldodecylimidazolium-*co*-4-styrene sulfonate)
TCM	Tricyanomethide
TCB	Tetracyanoborate
TfO	Trifluoromethanesulfonate
Tf_2N	Bis(trifluoromethylsulfonyl)imide
PF_6	Hexafluorophosphate
AIBN	2,2′-Azobis(2-methylpropionitrile)
APS	Ammonium persulfate
SMBS	Sodium metabisulfite
OD_{600}	Optical density at 600 nm
PC_i	Partition coefficient (eqn (1))
$\alpha_{i/w}$	Solute/water selectivity (eqn (2))
w_i^β	Concentration of component 'i' in phase 'β' ($g\ kg^{-1}$)

Conflicts of interest

There are no conflicts to declare.

Acknowledgements

We gratefully acknowledge the financial support of DuPont Canada and the Natural Sciences and Engineering Research Council of Canada.

References

1 N. Qureshi, *Biofuels, Bioprod. Biorefin.*, 2008, **2**, 319–330.
2 T. C. Ezeji, N. Qureshi and H. P. Blaschek, *Curr. Opin. Biotechnol.*, 2007, **18**, 220–227.
3 M. C. Grady, M. Jahic and R. Patnaik, *US* 2009/0305370Al, 2009.
4 W. A. Evanko *et al.*, *US* 8101808, 2012, 2.
5 B. Ndaba, I. Chiyanzu and S. Marx, *Biotechnol. Rep.*, 2015, **8**, 1–9.
6 T. Ezeji, C. Milne, N. D. Price and H. P. Blaschek, *Appl. Microbiol. Biotechnol.*, 2010, **85**, 1697–1712.
7 W. Van Hecke, G. Kaur and H. De Wever, *Biotechnol. Adv.*, 2014, **32**, 1245–1255.
8 J. T. Dafoe and A. J. Daugulis, *Biotechnol. Lett.*, 2014, **36**, 443–460.
9 G. Quijano, M. Hernandez, F. Thalasso, R. Muñoz and S. Villaverde, *Appl. Microbiol. Biotechnol.*, 2009, **84**, 829–846.
10 A. Arca-Ramos, G. Eibes, M. T. Moreira, G. Feijoo and J. M. Lema, *Chem. Eng. J.*, 2014, **240**, 281–289.

11 L. D. Collins and A. J. Daugulis, *Biotechnol. Bioeng.*, 1997, **55**, 155–162.
12 J. L. Rols, J. S. Condoret, C. Fonade and G. Goma, *Biotechnol. Bioeng.*, 1990, **35**, 427–435.
13 A. B. Pereiro, J. M. M. Araujo, J. M. S. S. Esperança, I. M. Marrucho and L. P. N. Rebelo, *J. Chem. Thermodyn.*, 2012, **46**, 2–28.
14 Y. Kohno and H. Ohno, *Chem. Commun.*, 2012, **48**, 7119–7130.
15 L. Y. Garcia-chavez, C. M. Garsia, B. Schuur and A. B. De Haan, *Ind. Eng. Chem. Res.*, 2012, **51**(24), 8293–8301.
16 H. R. Cascon, S. K. Choudhari, G. M. Nisola, E. L. Vivas, D. J. Lee and W. J. Chung, *Sep. Purif. Technol.*, 2011, **78**, 164–174.
17 S. H. Ha, N. L. Mai and Y.-M. Koo, *Process Biochem.*, 2010, **45**, 1899–1903.
18 R. Melgarejo-Torres, C. O. Castillo-Araiza, P. López-Ordaz, N. V. Calleja-Castañeda, J. L. Cano-Velasco, R. M. Camacho-Ruíz, G. J. Lye and S. Huerta-Ochoa, *Chem. Eng. J.*, 2015, **279**, 379–386.
19 O. Dipeolu, E. Green and G. Stephens, *Green Chem.*, 2009, **11**, 397.
20 M. Matsumoto, K. Mochiduki, K. Fukunishi and K. Kondo, *Sep. Purif. Technol.*, 2004, **40**, 97–101.
21 A. Romero, A. Santos, J. Tojo and A. Rodríguez, *J. Hazard. Mater.*, 2008, **151**, 268–273.
22 K. M. Docherty and C. F. Kulpa Jr., *Green Chem.*, 2005, **7**, 185.
23 A. G. Fadeev and M. M. Meagher, *Chem. Commun.*, 2001, 295–296.
24 F. Ganske and U. T. Bornscheuer, *Biotechnol. Lett.*, 2006, **28**, 465–469.
25 M. Matsumoto, K. Mochiduki and K. Kondo, *J. Biosci. Bioeng.*, 2004, **98**, 344–347.
26 G. Quijano, A. Couvert and A. Amrane, *Bioresour. Technol.*, 2010, **101**, 8923–8930.
27 R. J. Cornmell, C. L. Winder, S. Schuler, R. Goodacre and G. Stephens, *Green Chem.*, 2008, **10**, 685–691.
28 S. L. Bacon, A. J. Daugulis and J. S. Parent, *Green Chem.*, 2016, **18**, 6586–6595.
29 H. Zhao, O. Olubajo, Z. Song, A. L. Sims, T. E. Person, R. A. Lawal and L. A. Holley, *Bioorg. Chem.*, 2006, **34**, 15–25.
30 H. Zhao, *J. Mol. Catal. B: Enzym.*, 2005, **37**, 16–25.
31 M. C. Tomei, M. C. Annesini, S. Rita and A. J. Daugulis, *Environ. Sci. Technol.*, 2010, **44**, 7254–7259.
32 D. R. Nielsen and K. J. Prather, *Biotechnol. Bioeng.*, 2009, **102**, 811–821.
33 M. Montes, A. J. Daugulis, M. C. Veiga and C. Kennes, *J. Chem. Technol. Biotechnol.*, 2011, **86**, 47–53.
34 S. L. Bacon, A. J. Daugulis and J. S. Parent, *Chem. Eng. J.*, 2016, **299**, 56–62.
35 J. Yuan and M. Antonietti, *Polymer*, 2011, **52**, 1469–1482.
36 W. J. Horne, M. A. Andrews, K. L. Terrill, S. S. Hayward, J. Marshall, K. A. Belmore, M. S. Shannon and J. E. Bara, *ACS Appl. Mater. Interfaces*, 2015, **7**, 8979–8983.
37 W. Bi, B. Tang and K. H. Row, *Bioprocess Biosyst. Eng.*, 2013, **36**, 651–658.
38 B. Tang, W. Bi and K. H. Row, *Bioresour. Technol.*, 2013, **137**, 25–32.
39 W. Bi, M. Wang, X. Yang and K. H. Row, *J. Sep. Sci.*, 2014, **37**, 1632–1639.
40 H. Ohno and K. Ito, *Chem. Lett.*, 1998, **27**, 751–752.
41 S. B. Aher and P. R. Bhagat, *Res. Chem. Intermed.*, 2016, **42**(6), 5587–5596.
42 R. Marcilla, J. A. Blazquez, J. Rodriguez, J. A. Pomposo and D. Mecerreyes, *J. Polym. Sci., Part A: Polym. Chem.*, 2004, **42**, 208–212.
43 A. W. Mix and A. J. Giacomin, *J. Test. Eval.*, 2011, **39**, 1–10.
44 P. M. Doran and J. E. Bailey, *Biotechnol. Bioeng.*, 1986, **28**, 73–87.
45 L. D. Collins and A. J. Daugulis, *Appl. Microbiol. Biotechnol.*, 1999, **52**, 354–359.
46 R. Muñoz, M. Chambaud, S. Bordel and S. Villaverde, *Appl. Microbiol. Biotechnol.*, 2008, **79**, 33–41.
47 R. Muñoz, S. Arriaga, S. Hernández, B. Guieysse and S. Revah, *Process Biochem.*, 2006, **41**, 1614–1619.
48 S. Ostergaard, L. Olsson and J. Nielsen, *Microbiol. Mol. Biol. Rev.*, 2000, **64**, 34–50.
49 S. H. Park, S. Kim and J. S. Hahn, *Appl. Microbiol. Biotechnol.*, 2014, **98**, 9139–9147.
50 E. J. Steen, R. Chan, N. Prasad, S. Myers, C. J. Petzold, A. Redding, M. Ouellet and J. D. Keasling, *Microb. Cell Fact.*, 2008, **7**, 36.
51 J. E. Mark, *Polymer Data Handbook*, Oxford University Press, Cincinnati, 2nd edn, 1999.
52 M. Matsumura, H. Kataoka, M. Sueki and K. Araki, *Bioprocess Eng.*, 1988, **3**, 93–100.
53 W. E. Barton and A. J. Daugulis, *Appl. Microbiol. Biotechnol.*, 1991, **36**, 632–639.
54 W. R. Pitner, E. F. Aust, M. Schulte and U. Schmid-Grossmann, *WO* 2010000357, 2010.
55 US EPA, *Estimation Programs Interface Suite for Microsoft Windows*, 2015.
56 S. L. Bacon, J. S. Parent and A. J. Daugulis, *J. Chem. Technol. Biotechnol.*, 2014, **89**, 948–956.
57 S. L. Bacon, E. C. Peterson, A. J. Daugulis and J. S. Parent, *Biotechnol. Prog.*, 2015, **31**, 1500–1507.
58 J. S. Downey, G. McIsaac, R. S. Frank and H. D. H. Stöver, *Macromolecules*, 2001, **34**, 4534–4541.
59 K. Li and H. D. H. Stöver, *J. Polym. Sci., Part A: Polym. Chem.*, 1993, **31**, 2473–2479.
60 J. Qin, L. Bai, J. Wang, Y. Ma, H. Liu and S. He, *Anal. Methods*, 2014, **7**, 218–225.
61 Y. Wang, Q. L. Deng, G. Z. Fang, M. F. Pan, Y. Yu and S. Wang, *Anal. Chim. Acta*, 2012, **712**, 1–8.
62 A. Peterlin, *J. Macromol. Sci., Part B: Phys.*, 1975, **11**, 57–87.
63 A. Berthod, M. J. Ruiz-Ángel and S. Carda-Broch, *J. Chromatogr. A*, 2008, **1184**, 6–18.
64 M. K. Potdar, G. F. Kelso, L. Schwarz, C. Zhang and M. T. W. Hearn, *Molecules*, 2015, **20**, 16788–16816.

65 M. G. Freire, L. M. N. B. F. Santos, A. M. Fernandes, J. A. P. Coutinho and I. M. Marrucho, *Fluid Phase Equilib.*, 2007, **261**, 449–454.
66 H.-J. Huang, S. Ramaswamy and Y. Liu, *Sep. Purif. Technol.*, 2014, **132**, 513–540.
67 W. R. Pitner, M. Schulte, A. Gorak, F. Santangelo and A. E. Wentink, *WO* 2009152906, 2009.
68 N. Qureshi, S. Hughes, I. S. Maddox and M. a. Cotta, *Bioprocess Biosyst. Eng.*, 2005, **27**, 215–222.
69 J. Gmehling, J. Menke, J. Krafczyk, K. Fischer, J. Fontaine and H. V. Kehiaian, in *Handbook of chemistry and physics*, ed. D. R. Lide, CRC Press, Boca Raton, FL, 2005, pp. 6–160.